RP Current Trends in Engineering and Technology
Vol. 1, No. 6 (December 2022) pp. 137–145
e-ISSN: 2583-5491

RESEARCH PLATEAU PUBLISHERS

Cite this article: J. Gahlawat, Free and bound charge carrier's dependent Brillouin susceptibilities of weakly-piezoelectric magnetoactive semiconductors, *RP Cur. Tr. Eng. Tech.* **1** (2022) 137–145.

Original Research Article

Free and bound charge carrier's dependent Brillouin susceptibilities of weakly-piezoelectric magnetoactive semiconductors

Jyoti Gahlawat
Department of Physics, Baba Mastnath University, Asthal Bohar, Rohtak – 124021, Haryana, India
*Corresponding author, E-mail: jgahlawat.bmu@gmail.com

ARTICLE HISTORY
Received: 23 Oct. 2022
Revised: 29 Dec. 2022
Accepted: 30 Dec. 2022
Published online: 31 Dec. 2022

KEYWORDS
Brillouin susceptibility; III-V semiconductors, piezoelectricity, doping, magnetic field.

ABSTRACT
This study analyses the Brillouin susceptibilities of weakly piezoelectric, magnetoactive semiconductors depending on free and bound charge carriers. To generate formulas for the real and maginary parts of Brillouin susceptibilities, the coupled mode technique was applied. Under Voigt geometry, it is presumable that the semiconductor sample will be lit by an off-resonant pulsed laser. For numerical estimations, we choose n-type doped InSb crystal at liquid nitrogen temperature and illuminated by a pulsed CO_2 laser at 10.6 μm wavelength. To improve Brillouin susceptibilities and their sign change, efforts have been made to adjust the doping concentration, external magnetic field, and pump intensity. The ability of the chosen sample to serve as a potential candidate material for the fabrication of stimulated Brillouin scattering dependent widely tunable optoelectronic devices, such as optical switches and frequency converters, is confirmed by the change in sign of enhanced Brillouin susceptibilities in weakly piezoelectric semiconductors under the proper selection of n-type doping and external magnetic field.

1. Introduction

The fabrication of effective nonlinear optical (NLO) devices, such as optical frequency converters, optical amplifiers/oscillators, sensors [1, 2], optical signal processing, and pulse squeezing [3], depends on the results of experimental and analytical studies of NLO susceptibilities. These studies provide vital information about the optical properties of materials. Additionally, changes in the sign of NLO susceptibilities result in NLO phenomena including attenuation/amplification, self-defocusing/focusing, and optical amplifiers, optical limiters, and optical switches [4, 5].

The choice of an NLO medium and its operating frequency are both essential elements in the design and construction of effective NLO devices. Semiconductor crystals stand out among the numerous nonlinear optical media now in use for fabrication of NLO devices because [6, 7]: (i) The large number of mobile charge carriers (free electrons) present in doped semiconductors exhibit additional fascinating NLO phenomena; (ii) The relaxation time of carriers may be controlled by materials designing and device structuring; (iii) The observation of large magnitude NLO susceptibilities in close proximity to the band-gap resonant transition regimes; (iv) The use of changes in refractive index/ absorption coefficient; and (v) Operating the devices either optically or electrically

In addition to these benefits, doped semiconductor crystals exhibit a variety of optically excited coherent modes, such as plasmon mode, which results from plasma oscillations, acoustical phonon mode, which results from lattice vibrations, optical phonon mode, which results from molecular vibrations, polaron mode, which results from a conduction electron along with its self-induced polarisation, and polariton mode, which results from a strong interaction of a At the expense of coherent pump radiation, these coherent modes produce intriguing NLO events [8–10]. Due to its numerous technically significant applications in a variety of NLO devices and laser spectroscopy, stimulated Brillouin scattering (SRS), among other NLO phenomena, is currently one of the most prominent study topics [11]. SRS is a third-order NLO phenomenon that results from the medium's internally produced acoustical phonons scattering a coherent pump wave. SBS has been investigated in both the resonant and off-resonant transition regimes of semiconductor crystals [12, 13].

To improve the performance of NLO devices, semiconductor resonant Brillouin nonlinearities (SRBNs) have been used [14]. However, the SRBNs-based NLO devices have sluggish speeds. This is due to the fact that SRBNs are heavily dependent on energy build-up, carrier relaxation times, and population changes during the actual transition. The semiconductor non-resonant Brillouin nonlinearities (SNBNs), on the other hand, are typically smaller in size but exhibit a noticeably quick response time. They appear in the off-resonant transition phase. This is such that SNBNs do not require the establishment of new carriers or their relaxation.

Ultrafast optical switching devices are employed in contemporary digital optical communication systems, where signals are carried at high bit rates and high speeds. Despite the fabrication of many high refractive index NLO materials [15], there is still a strong need to investigate alternatives, particularly those that are compatible with semiconductor device technology, due to the rapid development of planar

devices like add-drop filters and wavelength division multiplexers/de-multiplexers in complex networks. Large optical nonlinearity coupled with quick response times at low pump fields is required to build high-speed compact optical switching systems with low power consumption. It is also preferred to choose materials with a very quick response time, minimal attenuation and absorption at the working frequency, low toxicity, and good mechanical and thermal stability.

The description above makes it very evident that SNBNs are crucial to today's high-speed digital communication systems. The improvement of SNBNs has been a key factor in raising the general performance of associated NLO devices. In the past, SNBNs and the performance of associated NLO devices have typically benefited from micro-structuring and compositing [16]. In addition to these, doping (free carriers) and externally applied electric/ magnetic fields can both affect semiconductor optical nonlinearities. These techniques have been used to understand the mechanics underlying a number of NLO events, including electro/magneto-optic effects [17]. When exposed to external electric and magnetic fields, many researchers [18–20] have found that a variety of III–V semiconductors' terahertz (THz) emission is significantly enhanced. Additionally, III-V semiconductors support a variety of vibrational modes and provide a variety of new scattering channels in the presence of external electric and magnetic fields, both of which have been applied to opto-acoustic diagnostics [21].

As far as the author is aware, there has never been a systematic investigation of how free and bound charge carriers affect Brillouin susceptibilities in weakly piezoelectric magnetised semiconductors. In the current research, we concentrated on the theoretical analysis of weakly piezoelectric magnetised semiconductors' Brillouin susceptibilities that depend on free and bound charge carriers. Expressions for real and imaginary parts of the free and bound charge carriers dependent Brillouin susceptibilities in weakly piezoelectric magnetoactive semiconducting crystals exposed to off-resonant laser irradiation have been developed using the coupled-mode theory [22]. For applications in rapid NLO devices, such as optical switches and frequency converters, efforts have been made to adjust the doping concentration and the external magnetic field to increase the magnitudes of Brillouin susceptibilities and change their sign. Finally, a set of data appropriate for weakly piezoelectric semiconductors (n-InSb) irradiated by a pulsed CO_2 laser at 10.6 μm wavelength has been used to make a thorough numerical explanation.

2. Objectives

The goal is to investigate the weakly piezoelectric magnetoactive semiconductors' free and bound charge carrier-dependent Brillouin susceptibilities and to determine the suitability of a chosen sample for the production of widely tunable stimulated Brillouin scattering-dependent optoelectronic devices like optical switches and frequency converters.

3. Theoretical formulations

In weakly piezoelectric magnetised semiconductors, free and bound charge carriers dependent Brillouin susceptibilities are discussed in this section. Three coherent electromagnetic fields' parametric coupling causes SBS to occur:
(i) an intense pump field $E_0(x,t) = E_0 \exp[i(k_0 x - \omega_0 t)]$,
(ii) an induced acoustic wave $u(x,t) = u_0 \exp[i(k_a x - \omega_a t)]$
(iii) a Stokes component of scattered pump field $E_s(x,t) = E_s \exp[i(k_s x - \omega_s t)]$.

The relations of energy and momentum conservation to be satisfied among these waves are: $\hbar\omega_0 = \hbar\omega_a + \hbar\omega_s$ and $\hbar\vec{k}_0 = \hbar\vec{k}_a - \hbar\vec{k}_s$, respectively.

In order to magnetize the weakly-piezoelectric semiconductor, we assume it be immersed in a static (or dc) magnetic field $\vec{B}_0 = \hat{z}B_0$ (i.e. perpendicular to wave vectors $\vec{k}_0$, $\vec{k}_a$ and $\vec{k}_s$). Such the field geometry is termed as 'Voigt geometry' [23]. In order to obtain expressions for Brillouin susceptibilities, the fluid model [24] has been used. This model imposes restrictions on the analysis and valid for $k_a l << 1$, where k_a is the acoustical phonon wave number, and l is the carriers mean free path.

The oscillating pump electromagnetic field generates density perturbations and derives an acoustical wave in the semiconductor crystal. Let x be the lattice position and $u(x, t)$ be the departure of lattice position from its original position so that one-dimensional strain in the direction of $+x$ axis (i.e. along the pump wave propagation direction) is given by $\partial u/\partial x$. Using Ref. [13], we may express the equation of motion of $u(x, t)$ as:

$$\frac{\partial^2 u}{\partial t^2} - \frac{C}{\rho}\frac{\partial^2 u}{\partial x^2} + 2\Gamma_a \frac{\partial u}{\partial t} = \frac{F_{eff}}{\rho}, \qquad (1a)$$

where C is the linear elastic modulus of the crystal such that the acoustical wave velocity is given by $v_a = (C/\rho)^{1/2}$. ρ represents the crystal mass density. In order to take account of acoustical damping, we introduced the term $2\Gamma_a(\partial u/\partial t)$ phenomenologically. F_{eff} stands for the net force per unit volume accomplished by the medium in the presence pump electromagnetic field, it can be expressed as [13]:

$F_{eff} = F^{(1)} + F^{(2)}$, where

$F^{(1)} = -\beta\frac{\partial E_{1s}}{\partial x}$ represents the first-order force arising due to piezoelectric property, and

$F^{(2)} = \frac{\gamma}{2}\frac{\partial}{\partial x}(E_0 E_{1s}^*)$ stands for second-order force arising due to electrostrictive property of weakly-piezoelectric semiconductor crystal.

Here β and γ are piezoelectric and electrostriction coefficients of the semiconductor medium, respectively. E_{1x} is the space charge electric field of the semiconductor medium. The complex entity's conjugate is indicated by an asterisk (*). It is important to note that the ions inside the lattice change into an asymmetrical position in the presence of an oscillating pump electromagnetic field, often causing a contraction in the direction of the pump field and an expansion in the direction perpendicular to the pump field direction. The electrostrictive force thus produced in the crystal is the source of the electrostrictive property. The medium experiences a piezoelectric force as a result of the electromagnetic field of an oscillating pump and the elastic characteristics of the lattice.

In the earlier studies, the origin of SBS has been taken into $F^{(2)}$; the contributions arising due to $F^{(1)}$ has normally been ignored. To examine free and bound charge carriers dependent Brillouin susceptibilities in weakly piezoelectric magnetised semiconductors, we integrated piezoelectricity's forces in the current analytical examination. After including the effects of piezoelectricity (substitution of F in Eq. (1a)), the modified equation of motion for $u(x, t)$ of lattice vibrations in a weakly-piezoelectric magnetized semiconductor crystal becomes

$$\frac{\partial^2 u}{\partial t^2} = \frac{C}{\rho}\frac{\partial^2 u}{\partial x^2} - 2\Gamma_a \frac{\partial u}{\partial t} - \frac{\beta}{\rho}\frac{\partial E_{1s}}{\partial x} + \frac{\gamma}{2\rho}\frac{\partial}{\partial x}(E_0 E_{1s}^*) . \quad (1b)$$

The other basic equations in the formulation of Brillouin susceptibilities are:

$$\frac{\partial \vec{v}_0}{\partial t} + \nu\vec{v}_0 + \left(\vec{v}_0 . \frac{\partial}{\partial x}\right)\vec{v}_0 = -\frac{e}{m}[\vec{E}_0 + (\vec{v}_0 \times \vec{B}_0)] \quad (2)$$

$$\frac{\partial \vec{v}_1}{\partial t} + \nu\vec{v}_1 + \left(\vec{v}_0 . \frac{\partial}{\partial x}\right)\vec{v}_1 + \left(\vec{v}_1 . \frac{\partial}{\partial x}\right)\vec{v}_0 = -\frac{e}{m}[\vec{E}_1 + (\vec{v}_0 \times \vec{B}_0)] \quad (3)$$

$$\frac{\partial n_1}{\partial t} + n_0\frac{\partial v_1}{\partial x} + n_1\frac{\partial v_0}{\partial x} + v_0\frac{\partial n_1}{\partial x} = 0 \quad (4)$$

$$\vec{P}_{es} = -\gamma\frac{\partial u^*}{\partial x}(\vec{E}_0) \quad (5)$$

$$\frac{\partial E_{1x}}{\partial x} + \frac{\beta}{\varepsilon}\frac{\partial^2 u}{\partial x^2} + \frac{\gamma}{\varepsilon}\frac{\partial^2 u^*}{\partial x^2}(E_0) = -\frac{n_1 e}{\varepsilon} . \quad (6)$$

These equations have been used by many researchers in theoretical studies of SBS in weakly-piezoelectric semiconductors. For detailed description of these equations, the reader is address to follow Ref. [13]. Here, n_0 ($\vec{v}_0$) and n_1 ($\vec{v}_1$) represent the equilibrium and perturbed carrier concentrations (oscillatory fluid velocities), respectively. ν stands for electron-electron collision frequency. m is the electron's effective mass. e is electronic charge. $\vec{P}_{es}$ stands for nonlinear polarization originating from acoustical vibrations derived by pump electromagnetic field.

The forces $F^{(1)}$ and $F^{(2)}$ generate carrier (here electrons) concentration perturbations in the semiconductor medium which can be obtained by using the method adopted by Aghamkar et al. [13]. We differentiate Eq. (4), substitute the value of E_{1x} from Eq. (6), first-order derivatives of v_0 and v_1 from Eqs. (2) and (3), respectively and after mathematical simplification obtained coupled equation of carrier density perturbations as

$$\frac{\partial^2 n_1}{\partial t^2} + \nu\frac{\partial n_1}{\partial t} + \bar{\omega}_p^2 n_1 + \frac{n_0 e k_s^2 u^*}{m\varepsilon_1}(\beta\gamma\delta_1\delta_2 A + \gamma^2 E_0^2)E_0 E_s^* = in_1 k_s \bar{E} \quad (7)$$

where $\bar{E} = \frac{e}{m}(\vec{E}_{eff})$, $A = \frac{\omega_p^2}{(e/m)k_a}$, $\bar{\omega}_p = \frac{\nu\omega_p}{(\nu^2 + \omega_c^2)^{1/2}}$,

$\delta_1 = 1 - \frac{\omega_c^2}{(\omega_0^2 - \omega_c^2)}$, $\delta_2 = 1 - \frac{\omega_c^2}{(\omega_s^2 - \omega_c^2)}$,

$\omega_c = \frac{eB_0}{m}$ (electron-cyclotron frequency), and

$\omega_p = \left(\frac{n_0 e^2}{m\varepsilon}\right)^{1/2}$ (electron-plasma frequency).

We may express the perturbed electron concentration n_1 as: $n_1 = n_{1s}(\omega_a) + n_{1f}(\omega_s)$, where n_{1s} (known as low frequency component) oscillates at acoustical wave frequency ω_a while n_{1f} (known as high frequency component) is associated with electromagnetic waves at frequencies $\omega_0 \pm p\omega_a$, in which p = 1, 2, 3, …. The electromagnetic fields at sum (i.e. $\omega_0 + p\omega_a$) and difference frequencies (i.e. $\omega_0 - p\omega_a$) are termed as anti-Stokes and Stokes modes, respectively. In the present analysis, we have neglected electron concentration fluctuations at off-resonant frequencies (with $p \geq 2$) and considered the first-order Stokes mode (with p = 1) only [13]. Under rotating-wave approximation (RWA), we obtained the following coupled equations from Eq. (7):

$$\frac{\partial^2 n_{1f}}{\partial t^2} + \nu\frac{\partial n_{1f}}{\partial t} + \bar{\omega}_p^2 n_{1f} + \frac{n_0 e k_s^2 u^*}{m\varepsilon_1}(\beta\gamma\delta_1\delta_2 A + \gamma^2 E_0^2)E_0 E_s^* = -in_{1s}^* k_s \bar{E} \quad (8a)$$

and

$$\frac{\partial^2 n_{1s}}{\partial t^2} + \nu\frac{\partial n_{1s}}{\partial t} + \bar{\omega}_p^2 n_{1s} = in_{1f}^* k_s \bar{E} . \quad (8b)$$

Eqs. (8a) and (8b) reveal that the slow and fast components (n_{1s}, n_{1f}) of the electron density perturbations are coupled to each other via the pump electromagnetic field ($\bar{E}$). Thus, it is clear that for SBS process to occur, the presence of the pump field is the fundamental necessity.

Solving the coupled wave equations (8a) and (8b) and using Eq. (1b), we obtained an expression for n_{1s} as

$$n_{1s} = \frac{\varepsilon_0 n_0 k_a k_s (\beta\gamma\delta_1\delta_2 A + \gamma^2 E_0^2)}{2\rho\varepsilon\delta_3(\Omega_a^2 + 2i\Gamma_a\omega_a)(\omega_0^2 - \omega_c^2 + 2i\nu\omega_0)} E_0 E_s^* , \quad (9)$$

where $\Omega_a^2 = \omega_a^2 - k_a^2 v_a^2$,

$\delta_3 = 1 - \frac{(\Omega_{ps}^2 - i\nu\omega_s)(\Omega_{pa}^2 + i\nu\omega_a)}{k_s^2 \bar{E}^2}$, in which

$\Omega_{ps}^2 = \bar{\omega}_p^2 - \omega_s^2$, and $\Omega_{pa}^2 = \bar{\omega}_p^2 - \omega_a^2$.

By ignoring the transition dipole moment, the Stokes component of induced current density resulting from nonlinear polarisation of a weakly piezoelectric magnetised doped semiconductor crystal may be written as follows:

$$J_{cd}(\omega_s) = n_{1s}^{*} e v_0 , \tag{10a}$$

which yields

$$J_{cd}(\omega_s) = \frac{\varepsilon_0 k_a k_s \omega_p^2 (\nu - i\omega_0)(\beta\gamma\delta_1\delta_2 A + \gamma^2 E_0^2)}{2\rho\delta_3(\Omega_a^2 + 2i\Gamma_a\omega_a)(\omega_0^2 - \omega_c^2 + 2i\nu\omega_0)} \left|E_0\right|^2 E_s^{*} . \tag{10b}$$

Weakly piezoelectric magnetised doped semiconductor crystal's nonlinear induced polarisation, which is a time integral of induced current density, can be stated as follows:

$$P_{cd}(\omega_s) = \int J_{cd}(\omega_s)\, dt = \frac{-J_{cd}(\omega_s)}{i\omega_s} , \tag{11a}$$

which yields

$$P_{cd}(\omega_s) = \frac{\varepsilon_0 k_a k_s \omega_p^2 \omega_0^3 (\beta\gamma\delta_1\delta_2 A + \gamma^2 E_0^2)}{2\rho\omega_s\delta_3(\Omega_a^2 + 2i\Gamma_a\omega_a)(\omega_0^2 - \omega_c^2 + 2i\nu\omega_0)} \left|E_0\right|^2 E_s^{*} . \tag{11b}$$

The induced polarization (at ω_s) due to induced current density may also be expressed as

$$P_{cd}(\omega_s) = \varepsilon_0 (\chi_B^{(3)})_{cd} \left|E_0\right|^2 E_s^{*} . \tag{11c}$$

We know that SBS is a third-order NLO process and hence the component of $P_{cd}(\omega_s)$ which is proportional to $\left|\bar{E}_0\right|^2 E_s^{*}$ yield free carrier dependent Brillouin susceptibility $(\chi_B^{(3)})_{cd}$. Comparing Eqs. (11b) and (11c), we obtain

$$(\chi_B^{(3)})_{cd} = \frac{k_a k_s \omega_p^2 \omega_0^3 (\beta\gamma\delta_1\delta_2 A + \gamma^2 E_0^2)}{2\rho\omega_s\delta_3(\Omega_a^2 + 2i\Gamma_a\omega_a)(\omega_0^2 - \omega_c^2 + 2i\nu\omega_0)} . \tag{12}$$

From Eq. (12), we observed that $(\chi_B^{(3)})_{cd}$ consists of following two parts:

(i) an intensity independent part $(\chi_B^{(3)})_{cd,Ii}$ (which occurs due to finiteness of both piezoelectricity β and electrostriction γ) given by

$$(\chi_B^{(3)})_{cd,Ii} = \frac{\beta\gamma\delta_1\delta_2 A k_a k_s \omega_p^2 \omega_0^3}{2\rho\omega_s\delta_3(\Omega_a^2 + 2i\Gamma_a\omega_a)(\omega_0^2 - \omega_c^2 + 2i\nu\omega_0)} , \tag{12a}$$

(ii) an intensity dependent part $(\chi_B^{(3)})_{cd,Id}$ (which occurs due to finiteness of piezoelectricity β only) given by

$$(\chi_B^{(3)})_{cd,Id} = \frac{\gamma^2 k_a k_s \omega_p^2 \omega_0^3 I}{\eta c\varepsilon_0\rho\omega_s\delta_3(\Omega_a^2 + 2i\Gamma_a\omega_a)(\omega_0^2 - \omega_c^2 + 2i\nu\omega_0)} , \tag{12b}$$

where $I = \frac{1}{2}\eta c\varepsilon_0 \left|E_0\right|^2$ is the pump wave intensity. η represents the background refractive index of medium and c is the speed of light.

Here, we mention that besides $P_{cd}(\omega_s)$, the weakly-piezoelectric magnetized semiconductor medium also possesses a polarization $P_{es}(\omega_s)$ having its origin in the interaction between pump wave and acoustical vibrational mode of the medium. Following Ref. [13], and using Eqs. (1) and (5), we obtain

$$P_{es}(\omega_s) = \frac{k_a k_s \omega_0^4 \gamma^2}{2\rho(\Omega_a^2 + 2i\Gamma_a\omega_a)(\omega_0^2 - \omega_c^2 + 2i\nu\omega_0)} \left|E_0\right|^2 E_s^{*} . \tag{13a}$$

The induced polarization (at ω_s) due to acoustical vibrations may also be expressed as

$$P_{es}(\omega_s) = \varepsilon_0 (\chi_B^{(3)})_{es} \left|E_0\right|^2 E_s^{*} . \tag{13b}$$

Comparing Eqs. (13a) and (13b), we obtain

$$(\chi_B^{(3)})_{es} = \frac{k_a k_s \omega_0^4 \gamma^2}{2\varepsilon_0\rho(\Omega_a^2 + 2i\Gamma_a\omega_a)(\omega_0^2 - \omega_c^2 + 2i\nu\omega_0)} . \tag{14}$$

From Eq. (14), we observed that $(\chi_B^{(3)})_{es}$ is independent of pump intensity and it occurs due to finiteness of electrostriction of the medium. Moreover, from Eqs. (12a), (12b) and (14), we observed that $(\chi_B^{(3)})_{cd,Ii}$, $(\chi_B^{(3)})_{cd,Id}$ and $(\chi_B^{(3)})_{es}$ are complex quantities. These can be put forward as:

$$(\chi_B^{(3)})_{cd,Ii} = [(\chi_B^{(3)})_{cd,Ii}]_r + i[(\chi_B^{(3)})_{cd,Ii}]_i ,$$

$$(\chi_B^{(3)})_{cd,Id} = [(\chi_B^{(3)})_{cd,Id}]_r + i[(\chi_B^{(3)})_{cd,Id}]_i , \text{ and}$$

$$(\chi_B^{(3)})_{es} = [(\chi_B^{(3)})_{es}]_r + i[(\chi_B^{(3)})_{es}]_i .$$

Here $[(\chi_B^{(3)})_{cd,Ii}]_r$ and $[(\chi_B^{(3)})_{cd,Ii}]_i$ represent the real and imaginary parts of intensity independent and free carrier dependent Brillouin susceptibility ($(\chi_B^{(3)})_{cd,Ii}$), respectively. Similarly $[(\chi_B^{(3)})_{cd,Id}]_r$ and $[(\chi_B^{(3)})_{cd,Id}]_i$ represent the real and imaginary parts of intensity dependent and free carrier dependent Brillouin susceptibility ($(\chi_B^{(3)})_{cd,Id}$), respectively. $[(\chi_B^{(3)})_{es}]_r$ and $[(\chi_B^{(3)})_{es}]_i$ stand for the real and imaginary parts of bound carrier dependent Brillouin susceptibility ($(\chi_B^{(3)})_{es}$), respectively.

Rationalizing Eqs. (12a), (12b) and (14), we obtain

$$[(\chi_B^{(3)})_{cd,Ii}]_r = \frac{\beta\gamma\delta_1\delta_2 A k_a k_s \omega_p^2 \omega_0^3 [\Omega_a^2(\omega_0^2 - \omega_c^2) - 4\nu\Gamma_a\omega_a\omega_0]}{2\rho\omega_s\delta_3(\Omega_a^4 + 4\Gamma_a^2\omega_a^2)[(\omega_0^2 - \omega_c^2)^2 + 4\nu^2\omega_0^2]} \tag{15}$$

$$[(\chi_B^{(3)})_{cd,Id}]_r = \frac{\gamma^2 k_a k_s \omega_p^2 \omega_0^3 I[\Omega_a^2(\omega_0^2 - \omega_c^2) - 4\nu\Gamma_a\omega_a\omega_0]}{\eta c\varepsilon_0\rho\omega_s\delta_3(\Omega_a^4 + 4\Gamma_a^2\omega_a^2)[(\omega_0^2 - \omega_c^2)^2 + 4\nu^2\omega_0^2]} \tag{16}$$

$$[(\chi_B^{(3)})_{cd,Ii}]_i = \frac{\beta\gamma\delta_1\delta_2 A k_a k_s \omega_p^2 \omega_0^3 [\Gamma_a\omega_a(\omega_0^2 - \omega_c^2) + \nu\omega_a^2\omega_0]}{2\rho\omega_s\delta_3(\Omega_a^4 + 4\Gamma_a^2\omega_a^2)[(\omega_0^2 - \omega_c^2)^2 + 4\nu^2\omega_0^2]} , \tag{17}$$

$$[(\chi_B^{(3)})_{cd,Id}]_i = \frac{\gamma^2 k_a k_s \omega_p^2 \omega_0^3 I[\Gamma_a\omega_a(\omega_0^2 - \omega_c^2) + \nu\omega_a^2\omega_0]}{\eta c\varepsilon_0\rho\omega_s\delta_3(\Omega_a^4 + 4\Gamma_a^2\omega_a^2)[(\omega_0^2 - \omega_c^2)^2 + 4\nu^2\omega_0^2]} \tag{18}$$

$$[(\chi_B^{(3)})_{es}]_r = \frac{k_a k_s \omega_0^4 \gamma^2 [\Omega_a^2(\omega_0^2-\omega_c^2) - 4\nu\Gamma_a\omega_a\omega_0]}{2\varepsilon_0\rho(\Omega_a^4+4\Gamma_a^2\omega_a^2)[(\omega_0^2-\omega_c^2)^2+4\nu^2\omega_0^2]}, \quad (19)$$

$$[(\chi_B^{(3)})_{es}]_i = \frac{k_a k_s \omega_0^4 \gamma^2 [\Gamma_a\omega_a(\omega_0^2-\omega_c^2) + \nu\omega_a^2\omega_0]}{2\varepsilon_0\rho(\Omega_a^4+4\Gamma_a^2\omega_a^2)[(\omega_0^2-\omega_c^2)^2+4\nu^2\omega_0^2]}. \quad (20)$$

Eqs. (15) – (20) show that $[(\chi_B^{(3)})_{cd,Ii}]_r$ and $[(\chi_B^{(3)})_{cd,Ii}]_i$ are influenced by β, γ, n_0 (via ω_p), and B_0 (via ω_c); $[(\chi_B^{(3)})_{cd,Id}]_r$ and $[(\chi_B^{(3)})_{cd,Id}]_i$ are influenced by γ, n_0 (via ω_p), B_0 (via ω_c), and I; $[(\chi_B^{(3)})_{es}]_r$ and $[(\chi_B^{(3)})_{es}]_i$ are influenced by γ, B_0 (via ω_c). In the forthcoming section, Eqs. (15) – (20) have been utilized for detailed analysis.

4. Results and discussion

In order to fulfill the condition viz. off-resonant laser irradiation, we choose n-type doped InSb crystal at liquid nitrogen temperature and illuminated by a pulsed CO_2 laser at 10.6 μm wavelength. At liquid nitrogen temperature,

(i) Since the weakly piezoelectric semiconductor medium's absorption coefficient is fairly low (about 10 m wavelength), band-to-band transition effects can be safely disregarded [25], and

(ii) Acoustical vibrations are the predominant scattering mechanism for electron energy and momentum transfer in weakly piezoelectric semiconductors [26].

Using Eqs. (15) – (20) for the material parameters of n-InSb [13], the Brillouin susceptibilities dependence on various parameters such as doping concentration n_0, external magnetic field B_0, and pump intensity (I) have been explored. Efforts have been targeted at:

(i) determination of appropriate values of n_0, B_0 and I to enhance Brillouin susceptibilities, and

(ii) searching the usefulness of fast NLO devices based on Brillouin nonlinearities.

An interesting feature of the present analysis is that for $E_0 < E_c (= 1.01\times10^8\ \mathrm{Vm^{-1}};\ \gamma^2E_0^2 < \beta\gamma\delta_1\delta_2 A$, i.e. on right hand side of Eq. (12), the first term inside the square bracket dominates over the second term and hence $(\chi_B^{(3)})_{cd,Id} < (\chi_B^{(3)})_{cd,Ii}$. For $E_0 > E_c$, $\beta\gamma\delta_1\delta_2 A < \gamma^2E_0^2$, i.e. on right hand side of Eq. (12), the second term inside the square bracket dominates over the first term and hence $(\chi_B^{(3)})_{cd,Ii} < (\chi_B^{(3)})_{cd,Id}$. At $E_0 = E_c$, $\gamma^2E_0^2 = \beta\gamma\delta_1\delta_2 A$ and hence $(\chi_B^{(3)})_{cd,Id} = (\chi_B^{(3)})_{cd,Ii}$.

The nonlinear absorption coefficient is accounted for by the imaginary part of Brillouin susceptibilities, while the nonlinear index of refraction of the selected NLO medium is accounted for by the real part. A variety of NLO devices, such as amplifiers, filters, and couplers, can be designed for an NLO medium with the use of knowledge of the nonlinear absorption coefficient and index of refraction [21].

In Figures 1a and 1b, $[(\chi_B^{(3)})_{cd,Ii}]_r$ and $[(\chi_B^{(3)})_{cd,Ii}]_i$ are plotted versus magnetic field B_0 for two different values of doping concentration ($n_0 = 2\times10^{19}\ \mathrm{m^{-3}}$ and $3\times10^{19}\ \mathrm{m^{-3}}$), respectively. These clearly show the substantial enhancements of $[(\chi_B^{(3)})_{cd,Ii}]_r$ and $[(\chi_B^{(3)})_{cd,Ii}]_i$ as well as alter of their sign. The situation at which $[(\chi_B^{(3)})_{cd,Ii}]_r$ and $[(\chi_B^{(3)})_{cd,Ii}]_i$ alter their sign is termed as 'cut-off' or 'dielectric anomaly' [27].

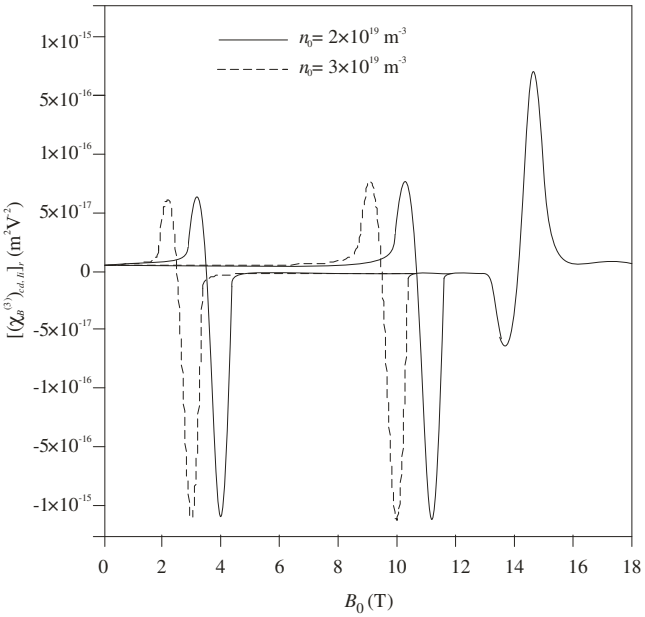

Figure 1a: Plot of $[(\chi_B^{(3)})_{cd,Ii}]_r$ versus B_0 for $n_0 = 2\times10^{19}$ and $3\times10^{19}\ \mathrm{m^{-3}}$.

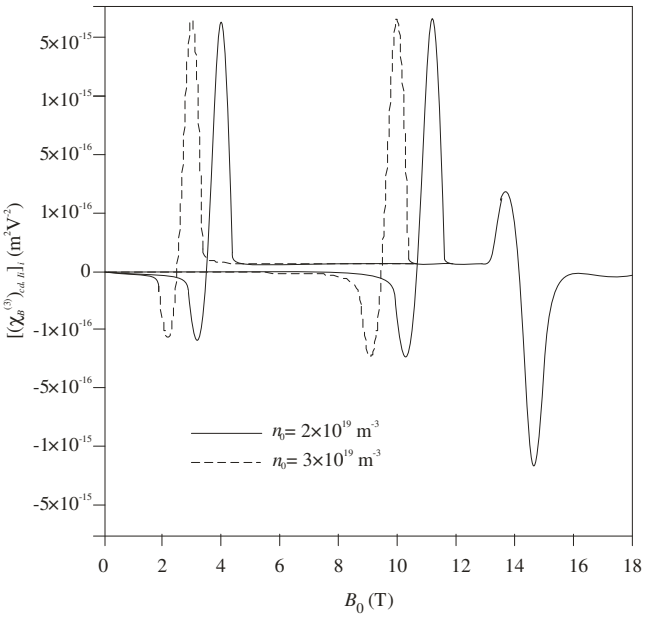

Figure 1b: Plot of $[(\chi_B^{(3)})_{cd,Ii}]_i$ versus B_0 for $n_0 = 2\times10^{19}$ and $3\times10^{19}\ \mathrm{m^{-3}}$.

By adjusting value of n_0 (say $2\times10^{19}\ \mathrm{m^{-3}}$) and varying B_0, we observed that $[(\chi_B^{(3)})_{cd,Ii}]_r$ is positive while $[(\chi_B^{(3)})_{cd,Ii}]_i$ is negative, vanishingly small and remain independent of magnetic field for $0 < B_0 < 2.5\,\mathrm{T}$. With further increasing B_0, $[(\chi_B^{(3)})_{cd,Ii}]_r$ starts increasing while $[(\chi_B^{(3)})_{cd,Ii}]_i$ starts decreasing, achieving a peak positive value ($[(\chi_B^{(3)})_{cd,Ii}]_r = +6.5\times10^{-17}\ \mathrm{m^2V^{-2}}$) and peak negative value ($[(\chi_B^{(3)})_{cd,Ii}]_i = -1.5\times10^{-16}\ \mathrm{m^2V^{-2}}$), respectively at $B_0 = 3.0\,\mathrm{T}$. With slightly increasing B_0 beyond this value, $[(\chi_B^{(3)})_{cd,Ii}]_r$ starts sharply decreasing while $[(\chi_B^{(3)})_{cd,Ii}]_i$ starts sharply increasing. At $B_0 = 3.5\,\mathrm{T}$, both $[(\chi_B^{(3)})_{cd,Ii}]_r$ as well as $[(\chi_B^{(3)})_{cd,Ii}]_i$ vanish. With further slightly increasing B_0 beyond this value, both $[(\chi_B^{(3)})_{cd,Ii}]_r$ as well as $[(\chi_B^{(3)})_{cd,Ii}]_i$ alter their

sign achieving a peak negative value ($[(\chi_B^{(3)})_{cd,Ii}]_r = -2.5\times10^{-15}$ m^2V^{-2}) and peak positive value ($[(\chi_B^{(3)})_{cd,Ii}]_i = +6.5\times10^{-15}\,m^2V^{-2}$) respectively at $B_0 = 4.0\,T$. For $4.0\,T < B_0 < 4.5\,T$, $[(\chi_B^{(3)})_{cd,Ii}]_r$ increases sharply while $[(\chi_B^{(3)})_{cd,Ii}]_i$ decreases sharply. For $4.5\,T < B_0 < 9.8\,T$, $[(\chi_B^{(3)})_{cd,Ii}]_r$ remains negative while $[(\chi_B^{(3)})_{cd,Ii}]_i$ remains positive and vanishingly small. With further increasing B_0 beyond this regime, again $[(\chi_B^{(3)})_{cd,Ii}]_r$ starts increasing while $[(\chi_B^{(3)})_{cd,Ii}]_i$ starts decreasing, achieving a peak positive value ($[(\chi_B^{(3)})_{cd,Ii}]_r = +7.5\times10^{-17}\,m^2V^{-2}$) and peak negative value $[(\chi_B^{(3)})_{cd,Ii}]_i = -2.5\times10^{-16}\,m^2V^{-2}$), respectively at $B_0 = 10.3\,T$. With slightly increasing B_0 beyond this value, again $[(\chi_B^{(3)})_{cd,Ii}]_r$ starts sharply decreasing while $[(\chi_B^{(3)})_{cd,Ii}]_i$ starts sharply increasing. At $B_0 = 10.8\,T$, both $[(\chi_B^{(3)})_{cd,Ii}]_r$ as well as $[(\chi_B^{(3)})_{cd,Ii}]_i$ vanish. With further slightly increasing B_0 beyond this value, again both $[(\chi_B^{(3)})_{cd,Ii}]_r$ as well as $[(\chi_B^{(3)})_{cd,Ii}]_i$ alter their sign achieving a peak negative value ($[(\chi_B^{(3)})_{cd,Ii}]_r = -2.5\times10^{-15}\,m^2V^{-2}$) and peak positive value ($[(\chi_B^{(3)})_{cd,Ii}]_i = +6.5\times10^{-15}\,m^2V^{-2}$) respectively at $B_0 = 11.3\,T$. For $11.3\,T < B_0 < 11.8\,T$, $[(\chi_B^{(3)})_{cd,Ii}]_r$ increases sharply while $[(\chi_B^{(3)})_{cd,Ii}]_i$ decreases sharply. For $11.8\,T < B_0 < 13.2\,T$, $[(\chi_B^{(3)})_{cd,Ii}]_r$ remains negative while $[(\chi_B^{(3)})_{cd,Ii}]_i$ remains positive and vanishingly small.

By adjusting value of n_0 at other value (say $3\times10^{19}\,m^{-3}$) and varying B_0, we observed that the features of the $[(\chi_B^{(3)})_{cd,Ii}]_r - B_0$ and $[(\chi_B^{(3)})_{cd,Ii}]_i - B_0$ plots remain unchanged except that the change of sign of $[(\chi_B^{(3)})_{cd,Ii}]_r$ and $[(\chi_B^{(3)})_{cd,Ii}]_i$ which were occurring at $B_0 = 3.5\,T$ and 10.8 T have now been shifted to $B_0 = 2.5\,T$ and 9.8 T, respectively. This distinct behavior of $[(\chi_B^{(3)})_{cd,Ii}]_r$ and $[(\chi_B^{(3)})_{cd,Ii}]_i$ occur due to following resonance conditions:

$$\text{(i)}\ \frac{\omega_p^2\omega_c^2}{\nu^2} \sim \omega_s^2, \text{ and (ii)}\ \frac{\nu^2\omega_p^2}{(\nu^2+\omega_c^2)} \sim \omega_s^2.$$

An exciting aspect of this resonance condition is the interaction between electron-cyclotron oscillator and electron-plasmon oscillator. We considered this as hybrid oscillator. When the pump electromagnetic field interacts with hybrid oscillator, as a consequence, electron-cyclotron and electron-plasma frequencies dependent Stokes signal is generated. It is beneficial to move the scattered Stokes wave frequency to an obtainable spectral regime in proportion to:

(i) ω_p (or n_0) for fixed ω_c (or B_0),
(ii) ω_c (or B_0) for fixed ω_p (or n_0), and
(iii) combination of ω_c and ω_p both.

By continuously increasing n_0 (via ω_p) and decreasing B_0 (via ω_c) in the same proportion maintains the resonance condition at a fixed value of ω_s. Further, by continuously increasing n_0 and decreasing B_0 without maintaining their proportion shifts the value of ω_s.

At $B_0 = 14.2\,T$, both $[(\chi_B^{(3)})_{cd,Ii}]_r$ as well as $[(\chi_B^{(3)})_{cd,Ii}]_i$ being independent of doping concentration alter their sign due to resonance between electron cyclotron frequency and pump wave frequency (i.e. $\omega_c^2 \sim \omega_0^2$).

In the proximity of resonance, the electron's drift velocity (which is the function of B_0) increases, attains a value higher than acoustical wave velocity and due to this the rate of energy flow from pump to acoustical wave increases, and consequently the amplification of acoustical wave occurs. Eventually, the interaction between pump electromagnetic field and amplified acoustical wave takes place and the amplitude of scattered Stokes mode enhances adequately.

The most significant feature of the result is monitoring of $[(\chi_B^{(3)})_{cd,Ii}]_r$ and $[(\chi_B^{(3)})_{cd,Ii}]_i$ by varying simultaneously/ independently n_0 and B_0 and also attaining large values of $[(\chi_B^{(3)})_{cd,Ii}]_r$ and $[(\chi_B^{(3)})_{cd,Ii}]_i$ in weakly-piezoelectric semiconductor crystals. The results obtained in Figures 1a and 1b permit the tuning of scattered Stokes mode over a broad frequency regime and reveal the opportunity of fabrication of frequency converters.

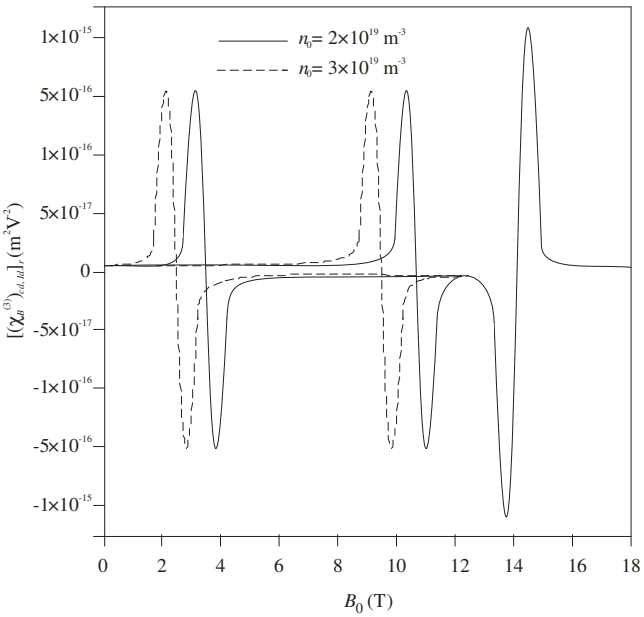

Figure 2a: Plot of $[(\chi_B^{(3)})_{cd,Id}]_r$ versus B_0 for $n_0 = 2\times10^{19}$ and 3×10^{19} m^{-3} at $I = 5.15\times10^{13}$ Wm^{-2}.

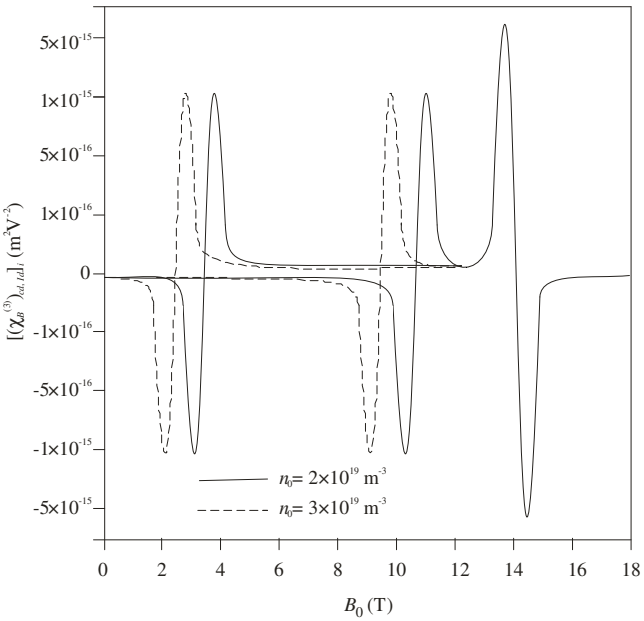

Figure 2b: Plot of $[(\chi_B^{(3)})_{cd,Id}]_i$ versus B_0 for $n_0 = 2\times10^{19}$ and 3×10^{19} m^{-3} at $I = 5.15\times10^{13}$ Wm^{-2}.

In Figures 2a and 2b, $[(\chi_B^{(3)})_{cd,Id}]_r$ and $[(\chi_B^{(3)})_{cd,Id}]_i$ are plotted versus magnetic field B_0 for two different values of doping concentration ($n_0 = 2\times10^{19}\,\mathrm{m^{-3}}$ and $3\times10^{19}\,\mathrm{m^{-3}}$) at $I = 5.15\times10^{13}\,\mathrm{Wm^{-2}}$, respectively. These give a picture of the enhancement of $[(\chi_B^{(3)})_{cd,Id}]_r$ and $[(\chi_B^{(3)})_{cd,Id}]_i$ as well as alter of their signs.

For $n_0 = 2\times10^{19}\,\mathrm{m^{-3}}$, we obtained positively enhanced value of $[(\chi_B^{(3)})_{cd,Id}]_r = +5.0\times10^{-16}\,\mathrm{m^2V^{-2}}$ and negatively enhanced value of $[(\chi_B^{(3)})_{cd,Id}]_i = -5.0\times10^{-16}\,\mathrm{m^2V^{-2}}$ at $B_0 = 3\,\mathrm{T}$ and 10.3 T; alter of their signs at $B_0 = 3.5\,\mathrm{T}$ and 10.8 T, and negatively enhanced value of $[(\chi_B^{(3)})_{cd,Id}]_r = -5.0\times10^{-16}\,\mathrm{m^2V^{-2}}$ and positively enhanced value of $[(\chi_B^{(3)})_{cd,Id}]_i = +5.0\times10^{-16}\,\mathrm{m^2V^{-2}}$ at $B_0 = 4.0\,\mathrm{T}$ and 11.3 T.

On the other hand, for $n_0 = 3\times10^{19}\,\mathrm{m^{-3}}$, we obtained positively enhanced value of $[(\chi_B^{(3)})_{cd,Id}]_r = +5.0\times10^{-16}\,\mathrm{m^2V^{-2}}$ and negatively enhanced value of $[(\chi_B^{(3)})_{cd,Id}]_i = -5.0\times10^{-16}\,\mathrm{m^2V^{-2}}$ at $B_0 = 2.0\,\mathrm{T}$ and 9.3 T; alter of their signs at $B_0 = 2.5\,\mathrm{T}$ and 9.8 T, and negatively enhanced value of $[(\chi_B^{(3)})_{cd,Id}]_r = -5.0\times10^{-16}\,\mathrm{m^2V^{-2}}$ and positively enhanced value of $[(\chi_B^{(3)})_{cd,Id}]_i = +5.0\times10^{-16}\,\mathrm{m^2V^{-2}}$ at $B_0 = 3.0\,\mathrm{T}$ and 10.3 T.

At $B_0 = 14.2\,\mathrm{T}$, both $[(\chi_B^{(3)})_{cd,Id}]_r$ as well as $[(\chi_B^{(3)})_{cd,Id}]_i$ being independent of doping concentration alter their sign from negative to positive and negative to positive respectively.

Based on the resonance circumstances already discussed in Figures 1a and 1b, this behaviour may be explained. With the help of these findings, optical switches and frequency converter manufacturing can be explored as well as the tuning of scattered Stokes waves over a broad frequency range.

A comparison between Figures 2a and 2b reveal that the nature of dependence of $[(\chi_B^{(3)})_{cd,Id}]_r$ and $[(\chi_B^{(3)})_{cd,Id}]_i$ on B_0 is differ not in magnitude but only in their sign; a case similar to Figures 1a and 1b. Note that apart from n_0 and B_0 dependence, intensity parameter can also be employed to enhance $[(\chi_B^{(3)})_{cd,Id}]_r$.

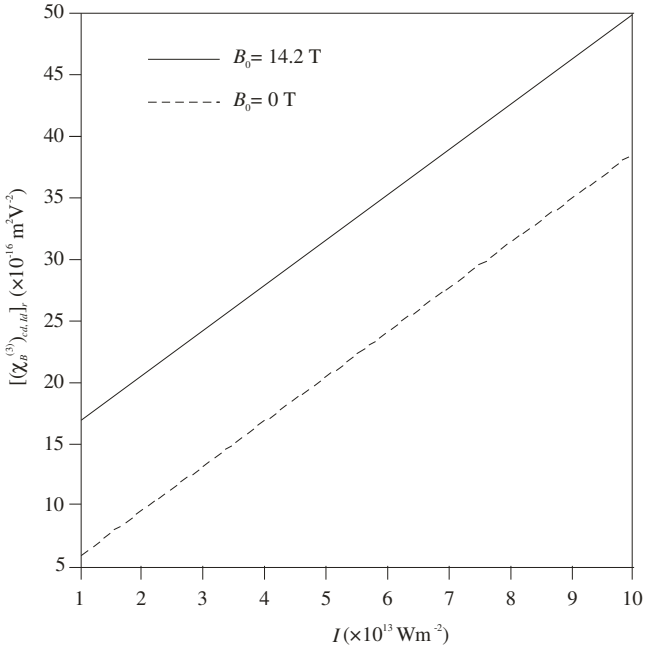

Figure 3a: Plot of $[(\chi_B^{(3)})_{cd,Id}]_r$ versus I for $B_0 = 0\,\mathrm{T}$ and 14.2 T at $n_0 = 3\times10^{19}\ \mathrm{m^{-3}}$.

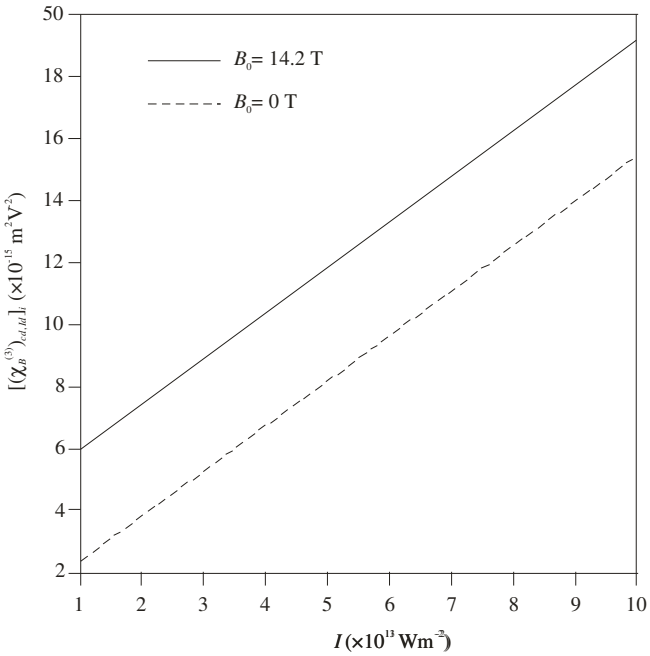

Figure 3b: Plot of $[(\chi_B^{(3)})_{cd,Id}]_i$ versus I for $B_0 = 0\,\mathrm{T}$ and 14.2 T at $n_0 = 3\times10^{19}\ \mathrm{m^{-3}}$.

In Figures 3a and 3b, both $[(\chi_B^{(3)})_{cd,Id}]_r$ and $[(\chi_B^{(3)})_{cd,Id}]_i$ are plotted versus pump intensity I for $B_0 = 0\,\mathrm{T}$ and 14.2T at $n_0 = 3\times10^{19}\,\mathrm{m^{-3}}$, respectively. It may be seen that for fixed values of both n_0 and B_0, the magnitudes of both $[(\chi_B^{(3)})_{cd,Id}]_r$ as well as $[(\chi_B^{(3)})_{cd,Id}]_i$ increase linearly with I. Moreover, for fixed n_0, both $[(\chi_B^{(3)})_{cd,Id}]_r$ as well as $[(\chi_B^{(3)})_{cd,Id}]_i$ are one order of magnitude higher at $B_0 = 14.2\,\mathrm{T}$ than at $B_0 = 0\,\mathrm{T}$. However, realistically an arbitrary increment in pump intensity may cause the optical damage of semiconductor crystal. When a semiconductor crystal is exposed to a long pulsed duration laser, a consequence is the generation of heat energy. Mayer et al. [28] pointed out that optical damage threshold of a semiconductor crystal may be decreased by the following methods: (i) method of free carrier nonlinear absorption, (ii) irradiating the sample by short pulsed duration laser.

In the present analysis, we considered the irradiation of weakly-piezoelectric semiconductor crystal by a nano-second pulsed CO_2 laser having pump intensity well below the optical damage threshold the sample.

In Figures 4a and 4b, $[(\chi_B^{(3)})_{es}]_r$ and $[(\chi_B^{(3)})_{es}]_i$ are plotted versus magnetic field B_0. It may be seen that initially $[(\chi_B^{(3)})_{es}]_r$ is negative while $[(\chi_B^{(3)})_{es}]_i$ is positive, vanishingly small ($\sim 10^{-19}\,\mathrm{m^2V^{-2}}$) and remains independent of magnetic field for $0 < B_0 < 14\,\mathrm{T}$. But when $B_0 = 14.2\,\mathrm{T}$ (i.e. $\omega_c^2 \sim \omega_0^2$), we obtained $[(\chi_B^{(3)})_{es}]_r, [(\chi_B^{(3)})_{es}]_i = \pm5.0\times10^{-17}\,\mathrm{m^2V^{-2}}$ and change of their signs occur at sharp resonance. Due to departure from resonance, $[(\chi_B^{(3)})_{es}]_r$ decreases while $[(\chi_B^{(3)})_{es}]_i$ increases sharply and achieve a comparatively smaller value. A comparison between Figures 4a and 4b reveal that the nature of dependence of $[(\chi_B^{(3)})_{es}]_r$ and $[(\chi_B^{(3)})_{es}]_i$ on B_0 is differ not in magnitude but only in their sign; a case similar to Figures 1a and 1b.

A comparison between results of Figures 1a, 1b and 4a, 4b reveal that free carrier dependent Brillouin susceptibilities are

two orders of magnitude higher than bound carrier dependent Brillouin susceptibilities.

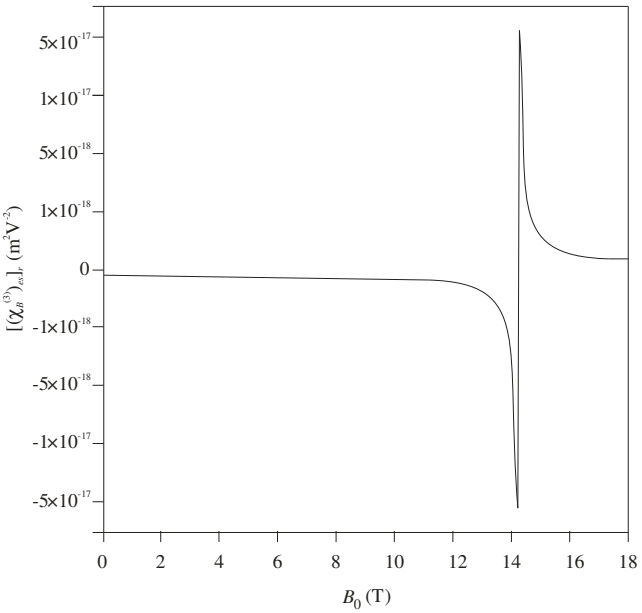

Figure 4a: Plot of $[(\chi_B^{(3)})_{es}]_r$ versus B_0.

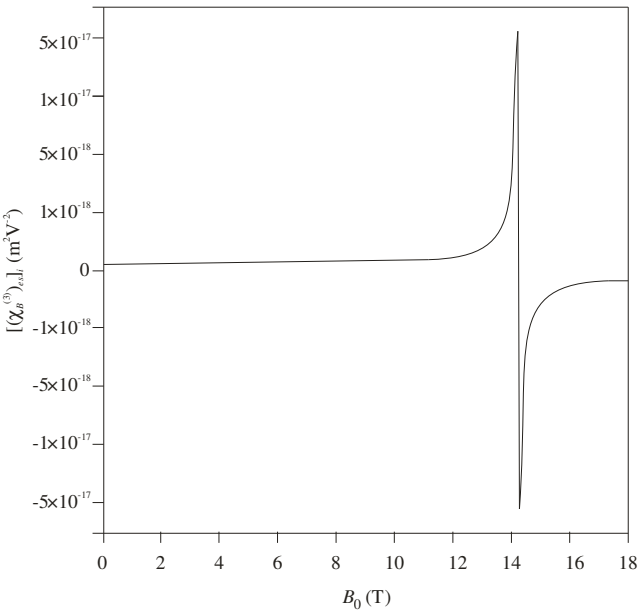

Figure 4b: Plot of $[(\chi_B^{(3)})_{es}]_i$ versus B_0.

5. Conclusions

In the current study, a numerical investigation of the dependent Brillouin susceptibilities of free and bound charge carriers in weakly piezoelectric magnetoactive semiconductor crystals is conducted. The Brillouin susceptibilities of magnetoactively doped semiconductors have been studied extremely successfully using the semiconductors fluid model, which takes into account both free and bound charge carriers. The analysis proposes three achievable resonance conditions for the dependent Brillouin susceptibilities of free carriers and only one achievable resonance condition for the dependent Brillouin susceptibilities of bound carriers, at which the Brillouin susceptibilities are enhanced and their sign is changed. The analysis also provides tuning of the scattered Stokes Brillouin mode that is free carrier dependent across a broad frequency range by altering the doping concentration and external magnetic field. Weakly piezoelectric, magnetoactive semiconductor crystals have been shown to have technological potential as extensively tunable optical switches and frequency converter hosts.

References

[1] H.J. Gerritsen, Image formation in phase conjugation with large wavelength conversion, *Appl. Phys. Lett*. **10** (1967) 239-241.

[2] B.I. Stepanov, E.V. Ivakin, A.G. Rubanov, On recording flat and volume dynamical holograms, *Dok. Acad. Nauk. SSSR* **196** (1971) 567.

[3] A. Yariv, P. Yeh, Optical Waves in Crystals, Wiley, New York (1984).

[4] G. Banfi, V. Degiorgio, D. Ricard, Nonlinear optical properties of semiconductor nanocrystals, *Adv. Phys*. **47** (1998) 447-510.

[5] H. Haug, S.W. Koch, Quantum Theory of the Optical and Electronic Properties of Semiconductors, 4th edn., World Scientific, Singapore (2004).

[6] D.A.B. Miller, Dynamic nonlinear optics in semiconductors: Physics and applications, *Laser Focus* **19** (1983) 61-68.

[7] R.K. Jain, Degenerate four-wave mixing in semiconductors: applications to phase conjugation and to picosecond resolved studies of transient carrier dynamics, *Opt. Eng*. **21** (1982) 199-218.

[8] Sandeep, S. Dahiya, N. Singh, Parametric excitation of optical phonons in weakly polar narrow band gap magnetized semiconductor plasmas, *Mod. Phys. Lett. B* **31** (2017) 1750294.

[9] S. Bhan, H.P. Singh, V. Kumar, M. Singh, Low threshold and high reflectivity of optical phase conjugate mode in transversely magnetized semiconductors, *Optik – Int. J. Light Electron Opt.* **184** (2019) 467-472.

[10] S. Jangra, H.P. Singh, V. Kumar, Acoustical-phonon and polaron mode-induced optical parametric amplification in transversely magnetized III-V semiconductors, *Mod. Phys. Lett. B* **33** (2019) 1950271.

[11] Z. Bai, H. Yuan, Z. Liu, P. Xu, Q. Gao, R.J. Williams, O. Kitzler, R.P. Mildren, Y. Wang, Z. Lu, Stimulated Brillouin scattering materials, experimental design and applications, *Opt. Mater*. **75** (2018) 626-645.

[12] P. Sen, P.K. Sen, Theory of stimulated Brillouin and Raman scattering in noncentrosymmetric crystals, *Phys. Rev. B* **31** (1985) 1034-1040.

[13] P. Aghamkar, M. Singh, N. Kishore, S. Duhan, P.K. Sen, Steady-state and transient Brillouin gain in magnetoactive narrow band gap semiconductors, *Semicond. Sci. Technol.* **22** (2007) 749-754.

[14] E. Garmire, Prospectives on stimulated Brillouin scattering, *New J. Phys*. **19** (2017) 011003.

[15] C.Y. Tai, J.S. Wilkinson, N.M.B. Perney, M.C. Netti, F. Cattaneo, C.E. Finlayson, J.J. Baumberg, Determination of nonlinear refractive index in a Ta_2O_5 rib waveguide using self-phase modulation, *Opt. Exp*. **12** (2004) 5110-5116.

[16] E. Garmire, Stimulated Brillouin review: invented 50 years ago and applied today, *Int. J. Opt*. **2018** (2018) Article ID 2459501.

[17] E. Garmire, Resonant optical nonlinearities in semiconductors, *IEEE J. Quantum Electron*. **6** (2000) 1094-1110.

[18] G. Meinert, L. Banyai, P. Gartner, H. Haug, Theory of THz emission from optically excited semiconductors in crossed electric and magnetic fields, *Phys. Rev. B* **62** (2000) 5003-5009.

[19] J.N. Heyman, P. Neocleous, D. Hebert, P.A. Crowell, T. Muller, K. Unterrainer, Terahertz emission from GaAs and InAs in a magnetic field, *Phys. Rev. B* **64** (2001) 85202.
[20] M.B. Johnston, D.M. Whittaker, A. Corchia, A.G. Davis, E.H. Linfield, Theory of magnetic-field enhancement of surface-field terahertz emission, *J. Appl. Phys*. **91** (2001) 2104-2106.
[21] V.E. Gusev, A.A. Karabutov, Laser Optoacoustics, American Institute of Physics, New York (1993).
[22] M.C. Pease, Generalized coupled mode theory, *J. Appl. Phys*. **32** (1961) 1736-1743.
[23] G.C. Aers, A.D. Boardman, The theory of semiconductor magnetoplasmon-polariton surface modes: Voigt geometry, *J. Phys. C: Solid State Phys*. **11** (1978) 945-959.
[24] S.G. Chefranov, A.S. Chefranov, Hydrodynamic Methods and Exact Solutions in Applications to the Electromagnetic Field Theory in Medium, in: Nonlinear Optics – Novel Results in Field Theory in Medium, B. Lembrikov (Ed.), Intechopen, U.K (2020).
[25] P.Y. Yu, M. Cardona, Vibrational Properties of Semiconductors, and Electron-Phonon Interactions, in: Fundamentals of Semiconductors. Graduate Texts in Physics, Springer, Berlin (2010).
[26] S.S. Li, Scattering Mechanisms and Carrier Mobilities in Semiconductors, in: Semiconductor Physical Electronics, S.S. Li (Ed.) Springer, New York (2006).
[27] E.D. Palik, J.K. Furdyna, Infrared and microwave magnetoplasma effects in semiconductors, *Rep. Prog. Phys*. **33** (1970) 1193-1322.
[28] J.M. Mayer, F.J. Bartoli, M.R. Kruer, Optical heating in semiconductors, *Phys. Rev. B* **21** (1980) 1559-1568.